

# Labdane-type Diterpenes from *Pinus eldarica* Needles and Their Anti-*Helicobacter pylori* Activity

Se Yun Jeong,<sup>#</sup> Myung Woo Na,<sup>#</sup> Eon Chung Park,<sup>#</sup> Jin-Chul Kim, Dong-Min Kang, Hamed Hamishehkar, Mi-Jeong Ahn, Jung Kyu Kim,<sup>\*</sup> and Ki Hyun Kim<sup>\*</sup>



Cite This: *ACS Omega* 2022, 7, 29502–29507



Read Online

ACCESS |



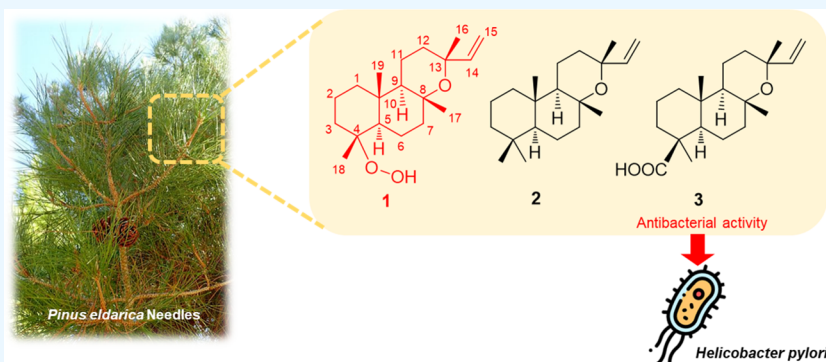
Metrics & More



Article Recommendations



Supporting Information



**ABSTRACT:** *Pinus eldarica* is a medicinal tree used in traditional herbal medicine for the treatment of bronchial asthma and various skin diseases. As part of our ongoing search for bioactive phytochemicals with novel structures in natural products, we performed a phytochemical analysis of the methanol (MeOH) extract from *P. eldarica* needles collected in Iran. Phytochemical investigation of the MeOH extract, aided by liquid chromatography–mass spectrometry-based analysis, resulted in the isolation and identification of three labdane-type diterpenes (1–3), including a new and relatively unique norlabdane-type diterpene with a peroxide moiety, eldaricoxide A (1). The chemical structures of the isolated labdane-type diterpenes were elucidated by analyzing the spectroscopic data from 1D and 2D NMR and high-resolution electrospray ionization–mass spectrometry. The absolute configuration of eldaricoxide A (1) was established by employing a computational method, including electronic circular dichroism calculation and specific optical rotation. An anti-*Helicobacter pylori* test was conducted, where compound 3 exhibited the most potent antibacterial activity against *H. pylori* strain 51, inducing 72.7% inhibition (MIC<sub>50</sub> value of 92 μM), whereas eldaricoxide A (1) exhibited moderate antibacterial activity against *H. pylori* strain 51, inducing 54.5% inhibition (MIC<sub>50</sub> value of 95 μM). These findings demonstrated that the identified bioactive labdane-type diterpenes 1 and 3 can be applied in the development of novel antibiotics against *H. pylori* for the treatment of gastric and duodenal ulcers.

## 1. INTRODUCTION

*Pinus eldarica* is an evergreen tree, originally from the Transcaucasian region of Europe and Asia and also found in Iran, Afghanistan, and Pakistan.<sup>1</sup> This species had been introduced to Iran several centuries ago, and it is particularly known for its ability to tolerate air contamination, dust, drought, and cold.<sup>2</sup> *P. eldarica* belongs to the family “Pinaceae,” characterized by a gray shell, needle-shaped leaves (pine needles), and single or paired cones.<sup>3</sup> Needles of pines belonging to Pinaceae have been known to contain phenolic compounds, such as catechin, epicatechin, and taxifolin, and the extracts of pine needles have been shown to exhibit diverse physiological and pharmacological actions,<sup>4</sup> such as anti-inflammatory,<sup>5</sup> anti-oxidant,<sup>6</sup> anti-neoplastic,<sup>7</sup> and immunomodulatory properties.<sup>7</sup> *P. eldarica* needles, buds, resins, and nuts have been widely used in traditional medicine for the

treatment of bronchial asthma and various skin diseases, such as wounds, allergic rashes, and dermatitis.<sup>8,9</sup>

Recent phytochemical analyses of *P. eldarica* showed that the essential oils extracted from its needles, fruit, bark, and pollen mainly consist of mono- and sesquiterpenoids, such as  $\alpha$ -pinene, caryophyllene oxide,  $\delta$ -3-carene, (*E*)- $\beta$ -caryophyllene, D-germacrene, longifolene, limonene, and myrtenal.<sup>3,10</sup> Pharmacological studies on *P. eldarica* extracts showed the potentiality of diverse therapeutic efficacies that can be

Received: July 1, 2022

Accepted: August 5, 2022

Published: August 15, 2022



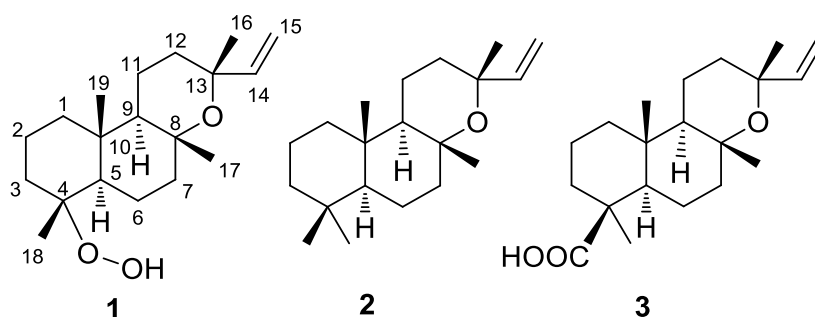


Figure 1. Chemical structures of compounds 1–3.

employed. For example, aqueous extracts from fruits exhibited anti-urolithiatic activity by inhibiting calcium oxalate deposition in rats with calcium oxalate nephrolithiasis;<sup>11</sup> nut extracts lowered blood cholesterol levels and decreased aortic atherosclerosis in hypercholesterolemic rabbits;<sup>12</sup> bark extracts exerted an anti-pseudomonas effect<sup>13</sup> and cytoprotective and genoprotective effects on human umbilical vein endothelial cells (HUVECs) following exposure to cisplatin;<sup>14</sup> and the needle extracts showed antidepressant activity in rats with reserpine-induced depression-like behavior,<sup>15</sup> a neuroprotective effect in a mouse model with pentylenetetrazole-induced seizure,<sup>16</sup> and anti-inflammatory effects by decreasing acute and chronic pain and inflammation.<sup>17</sup> Although there have been extensive pharmacological studies on *P. eldarica* extracts, the potential phytochemicals of *P. eldarica* have not received considerable attention.

As part of our ongoing natural product discovery of bioactive phytochemicals from diverse natural resources,<sup>18–23</sup> we investigated a methanol (MeOH) extract of *P. eldarica* needles collected in Iran to explore antibacterial diterpenes using the liquid chromatography–mass spectrometry (LC–MS)-based analysis. The chemical structures of the isolated diterpenes were elucidated using the conventional spectroscopic data analysis, including 1D and 2D nuclear magnetic resonance (NMR) and high-resolution electrospray ionization-mass spectrometry (HR-ESIMS) and computational methods for electronic circular dichroism (ECD) calculations and specific optical rotation. Herein, we described the isolation and structural elucidation of the isolated diterpenes 1–3 and evaluation of their anti-*Helicobacter pylori* activity.

## 2. RESULTS AND DISCUSSION

### 2.1. Isolation of Diterpenes from *P. eldarica* Needles.

The MeOH extract of *P. eldarica* needles was fractionated by solvent partition, which afforded the hexane-,  $\text{CH}_2\text{Cl}_2$ -, EtOAc-, and BuOH-soluble fractions. Each fraction was further subjected to LC–MS analysis, referencing an in-house UV library database in our LC–MS system, which revealed that the hexane-soluble fraction mainly contains diterpenes, which was also confirmed by thin layer chromatography (TLC) analysis. In addition, recent studies have reported that labdane diterpenoids and clerodane diterpenes isolated from *Andrographis paniculata* and *Polyalthia longifolia* leaves, respectively, exhibited anti-*H. pylori* activities,<sup>24,25</sup> indicating the potential of diterpenes as antimicrobial agents against *H. pylori*. Based on these results and preliminary data, the hexane-soluble fraction was subjected to phytochemical examination via repeated column chromatography and semipreparative high-performance liquid chromatography (HPLC) under the guidance of

LC–MS analysis, resulting in the isolation of three labdane-type diterpenes (1–3), including a new norlabdane-type diterpene (1) (Figure 1).

**2.2. Structural Elucidation of the Isolated Diterpenes 1–3.** Compound 1 was isolated as an amorphous white powder, and its molecular formula was determined to be  $\text{C}_{19}\text{H}_{32}\text{O}_3$ , deduced by the positive-ion mode of HR-ESIMS, which revealed an  $[\text{M} + \text{Na}]^+$  ion peak at  $m/z$  331.2250 (calcd for  $\text{C}_{19}\text{H}_{32}\text{O}_3\text{Na}$ , 331.2249). The established molecular formula for compound 1 exhibits 4 degrees of unsaturation. The  $^1\text{H}$  NMR data (Table 1) of compound 1, assigned with the aid of a heteronuclear single quantum correlation (HSQC) experiment, revealed the presence of characteristic signals for one terminal vinyl group at  $\delta_{\text{H}}$  5.87 (1H, dd,  $J = 17.5, 10.5$  Hz, H-14), 5.14 (1H, dd,  $J = 17.5, 1.5$  Hz, H-15b), and 4.92 (1H,

Table 1.  $^1\text{H}$  (850 MHz) and  $^{13}\text{C}$  NMR (212.5 MHz) Data for Compound 1 in  $\text{CDCl}_3$  ( $\delta$  ppm)<sup>a</sup>

position	$\delta_{\text{H}}$ ( $J$ in Hz)	$\delta_{\text{C}}^b$
1 $\alpha$	1.65, m	38.5 CH <sub>2</sub>
1 $\beta$	0.89, m	
2 $\alpha$	1.43, m	17.5 CH <sub>2</sub>
2 $\beta$	1.74, m	
3 $\alpha$	2.13, m	34.9 CH <sub>2</sub>
3 $\beta$	1.17, m	
4		84.0 C
5	1.20, m	55.9 CH
6 $\alpha$	1.81, m	19.7 CH <sub>2</sub>
6 $\beta$	1.47, m	
7 $\alpha$	1.38, m	43.1 CH <sub>2</sub>
7 $\beta$	1.84, m	
8		74.9 C
9	1.32, m	55 CH
10		37.1 C
11 $\alpha$	1.58, m	15.4 CH <sub>2</sub>
11 $\beta$	1.49, m	
12 $\alpha$	1.77, m	35.5 CH <sub>2</sub>
12 $\beta$	1.63, m	
13		73.5 C
14	5.87, dd (17.5, 10.5)	147.6 CH
15a	4.92, dd (10.5, 1.5)	110.3 CH <sub>2</sub>
15b	5.14, dd (17.5, 1.5)	
16	1.27, s	28.4 CH <sub>3</sub>
17	1.31, s	25.1 CH <sub>3</sub>
18	1.28, s	24.3 CH <sub>3</sub>
19	0.88, s	14.9 CH <sub>3</sub>

<sup>a</sup>Coupling constants (Hz) are given in parentheses. <sup>b</sup> $^{13}\text{C}$  NMR data are assigned based on HSQC and HMBC experiments.

dd,  $J = 10.5, 1.5$  Hz, H-15a) and four methyl groups at  $\delta_{\text{H}}$  1.31 (s, H-17), 1.28 (s, H-18), 1.27 (s, H-16), and 0.88 (s, H-19). The  $^{13}\text{C}$  NMR data (Table 1) of compound **1**, combined with a heteronuclear multiple bond correlation (HMBC) experiment, revealed 19 carbon resonances, including 4 non-protonated carbons at  $\delta_{\text{C}}$  37.1 (C-10), 73.5 (C-13), 74.9 (C-8), and 84.0 (C-4). Extensive inspection of the NMR data of compound **1** showed close resemblance to that of 4 $\alpha$ -hydroxy-18-normanoyl oxide, a norlabdane-type diterpene with evident variations in one aliphatic proton [ $\delta_{\text{H}}$  2.18 (H-3 $\alpha$ )] and two methyl groups [ $\delta_{\text{H}}$  1.28 (H-18) and 0.88 (H-19)] and a relatively high downfield-shifted carbon chemical shift value [ $\delta_{\text{C}}$  84.0 (C-4)] in compound **1**,<sup>26,27</sup> which indicated that compound **1** has a different unit at C-4 from the known compound, 4 $\alpha$ -hydroxy-18-normanoyl oxide.

The planar structure of compound **1** was elucidated by interpretation of 2D NMR, including  $^1\text{H}$ – $^1\text{H}$  correlated spectroscopy (COSY) and HMBC experiments. The key  $^1\text{H}$ – $^1\text{H}$  COSY and HMBC correlations (Figure 2) confirmed

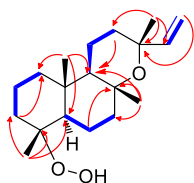


**Figure 2.** Key  $^1\text{H}$ – $^1\text{H}$  COSY (blue—) and HMBC (red↷) correlations for **1**.

the position of the methyl groups in the norlabdane-type diterpene of compound **1**, and the position of the terminal vinyl group was determined at C-13 by the HMBC correlations of H-15/C-13, H-16/C-12, C-13, and C-14 (Figure 2). Notably, the carbon chemical shift of C-4 in compound **1** ( $\delta_{\text{C}}$  84.0) was relatively downfield-shifted compared to that ( $\delta_{\text{C}}$  72.1) of 4 $\alpha$ -hydroxy-18-normanoyl oxide (C<sub>19</sub>H<sub>32</sub>O<sub>2</sub>).<sup>27</sup> Considering the established molecular formula for compound **1**, C<sub>19</sub>H<sub>32</sub>O<sub>3</sub>, deduced by HR-ESIMS and characteristic chemical shifts of  $\delta_{\text{H}}$  2.18 (H-3 $\alpha$ ) and  $\delta_{\text{C}}$  84.0 (C-4),<sup>26</sup> compound **1** was determined to have a peroxide group at C-4, instead of a hydroxyl group.

The relative configuration of compound **1** was established via nuclear Overhauser effect spectroscopy (NOESY) analysis. The NOESY correlations from H-19 to H-16, H-17, and H-18 confirmed that the corresponding methyl groups have same orientation (Figure 3), and the peroxide group at C-4 has opposite orientation. The NOESY cross-peaks from H-9 to H-

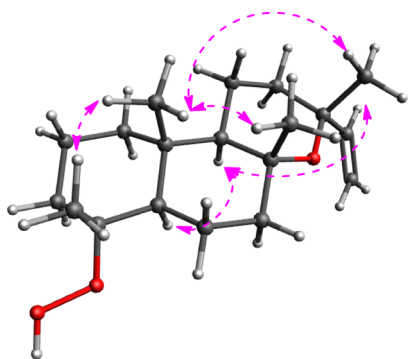


**Figure 3.** Key NOESY correlations of **1**.

5 and H-14 indicated that the corresponding protons have opposite configurations to the methyl groups at C-16, C-17, C-18, and C-19 (Figure 3).

Finally, the absolute configuration of compound **1** was confirmed by quantum chemical calculations for ECD simulations and comparison of optical rotation values. Two possible isomers, **1a** (4*R*,5*R*,8*R*,9*R*,10*R*,13*R*) and **1b** (4*S*,5*S*,8*S*,9*S*,10*S*,13*S*), were calculated for the ECD data, and the experimental ECD spectrum of compound **1** was compared with the obtained ECD data (Figure 4). The

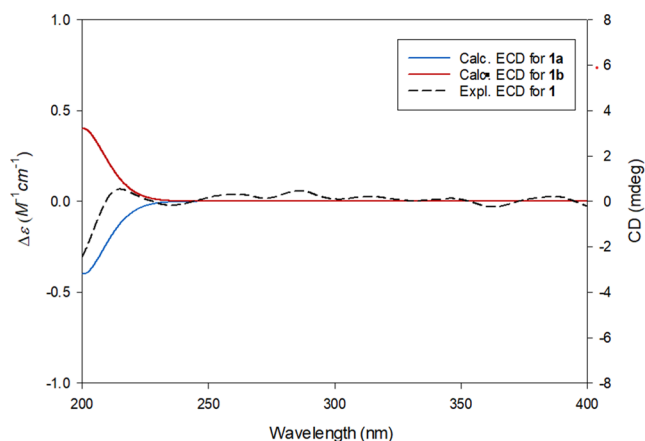


**Figure 4.** Experimental and calculated ECD spectra of compound **1**.

experimental ECD data highly correlated with the obtained ECD data of **1a**, which confirmed the absolute configuration of compound **1** as 4*R*,5*R*,8*R*,9*R*,10*R*,13*R*. The stereochemistry of compound **1** was also confirmed by the optical rotation values obtained for **1** ( $[\alpha]_{\text{D}}^{25} + 8.9$  (c 0.10, CHCl<sub>3</sub>)) and 4 $\alpha$ -hydroxy-18-normanoyl oxide ( $[\alpha]_{\text{D}}^{27} + 9.6$  (c 0.08, CHCl<sub>3</sub>)). Therefore, the chemical structure of **1**, including its absolute configuration, was determined as shown in Figure 1, designated eldaricoxide A. Although the representative sesquiterpene with the peroxide group, artemisinin, has been noted, the norlabdane-type diterpene (**1**) with the peroxide group was one of the relatively unique natural products.

The other isolated compounds were identified as (+)-manoyl oxide (**2**)<sup>28</sup> and manoyl oxide acid (**3**)<sup>29</sup> (Figure 1) by comparing their NMR spectral and physical data with those reported earlier and the data from LC–MS analysis.

**2.3. Evaluation of Antibacterial Activity of the Isolated Diterpenes against *H. pylori*.** *H. pylori* infection is a major public health challenge, affecting approximately 50% of the global population.<sup>30</sup> Eradication of *H. pylori* can help in the treatment of gastric and duodenal ulcers and gastric cancer since *H. pylori* is known to be the causative agent associated with several gastric and duodenal pathologies.<sup>31</sup> As aforementioned, recent studies have reported that several labdane-type diterpenoids exhibit anti-*H. pylori* activity.<sup>24</sup> Thus, the isolated labdane-type diterpenes **1**–**3** obtained in this study were evaluated for their antibacterial activity against *H. pylori* strain 51 (Table 2). Among the isolates, compound **3** exhibited the most potent antibacterial activity against *H. pylori* strain 51, inducing 72.7% inhibition at a final concentration of 100  $\mu\text{M}$ , comparable to that of metronidazole (97.0% inhibition) as a positive control, and it showed an MIC<sub>50</sub> value of 92  $\mu\text{M}$ . The novel compound **1** exhibited moderate antibacterial activity against *H. pylori* strain 51, inducing 54.5% inhibition, which



**Table 2. Anti-*H. pylori* Activity of Compounds 1–3 against *H. pylori* Strain 51 Treated with 100  $\mu\text{M}$  of Each Compound**

compounds	inhibition (%)	MIC <sub>50</sub> ( $\mu\text{M}$ )	MIC <sub>90</sub> ( $\mu\text{M}$ )
1	54.5	95	>100
2	26.8	>100	>100
3	72.7	92	>100
quercetin <sup>a</sup>	34.4	>100	>100
metronidazole <sup>a</sup>	97.0	17	46

<sup>a</sup>Positive controls.

was higher than that of quercetin (34.4% inhibition) as a positive control, and it showed an MIC<sub>50</sub> value of 95  $\mu\text{M}$ . Compound 2 exhibited weak activity against *H. pylori* strain 51, inducing 26.8% inhibition (Table 2). Based on these findings, the presence of carboxyl and peroxide groups at C-4 in the labdane-type diterpenes may be significant in the anti-*H. pylori* activity, with the carboxyl group appearing to have a more positive effect. Further studies are required to elucidate the mechanism by which compound 3 inhibits *H. pylori* growth.

### 3. CONCLUSIONS

In this study, phytochemical investigation of the MeOH extract of *P. eldarica* needles collected in Iran resulted in the isolation and identification of a novel norlabdane-type diterpene (1) with a peroxide moiety and two known labdane-type diterpenes (2 and 3). Manoyl oxide acid (3) exhibited the most potent antibacterial activity against *H. pylori* strain 51, inducing 72.7% inhibition (MIC<sub>50</sub> value of 92  $\mu\text{M}$ ), while eldaricoxide A (1) exhibited moderate antibacterial activity against *H. pylori* strain 51, inducing 54.5% inhibition (MIC<sub>50</sub> value of 95  $\mu\text{M}$ ). It has been reported that four labdane-type diterpenes inhibited the growth of *H. pylori* via inhibition of urease.<sup>24</sup> Further study is required to elucidate the exact mechanism of compounds 2 and 3 to inhibit the growth of *H. pylori*. In addition, specificity toward *H. pylori* including antibacterial activity against other pathogenic bacteria and toxicity of these compounds is also required in the following study. This study provides experimental evidence that bioactive labdane-type diterpenes can serve as natural antibacterial agents against *H. pylori*.

### 4. EXPERIMENTAL SECTION

**4.1. General Experimental Procedures.** Optical rotations were measured using a JASCO P-2000 polarimeter (JASCO, Easton, MD, USA). Ultraviolet (UV) spectra were obtained using an Agilent 8453 UV–visible spectrophotometer (Agilent Technologies, Santa Clara, CA, USA). The ECD spectra were obtained using a JASCO J-1500 spectropolarimeter (JASCO). Infrared (IR) spectra were obtained using a Bruker IFS-66/S FT-IR spectrometer (Bruker, Karlsruhe, Germany). NMR spectra were obtained using a Bruker AVANCE III HD 850 NMR spectrometer with a 5 mm TCI CryoProbe operating at 850 MHz (<sup>1</sup>H) and 212.5 MHz (<sup>13</sup>C), with chemical shifts given in ppm ( $\delta$ ) for <sup>1</sup>H and <sup>13</sup>C NMR analyses. All HR-ESIMS data were obtained using an Agilent G6545B quadrupole time-of-flight mass spectrometer (Agilent Technologies) coupled to an Agilent 1290 Infinity II HPLC instrument using an Agilent Eclipse Plus C18 column (2.1  $\times$  50 mm, 1.8  $\mu\text{m}$ ; flow rate: 0.3 mL/min). Preparative HPLC was performed using a Waters 1525 Binary HPLC pump with a Waters 996 photodiode array detector (Waters Corporation, Milford, MA, USA) and a Hecor C18 column (250  $\times$  21.2

mm, 5  $\mu\text{m}$ ; flow rate: 5 mL/min; Rstech Corporation, Korea). Semipreparative HPLC was performed using a Shimadzu Prominence HPLC System with SPD-20A/20AV Series Prominence HPLC UV–vis detectors (Shimadzu, Tokyo, Japan) and a Phenomenex Luna phenyl-hexyl column (250  $\times$  10 mm, 5  $\mu\text{m}$ ; flow rate, 2 mL/min; Phenomenex, Torrance, CA, USA). The LC–MS analysis was performed using an Agilent 1200 Series HPLC system equipped with a diode array detector and 6130 Series ESI mass spectrometer using an analytical Kinetex C18 100 Å column (100  $\times$  2.1 mm, 5  $\mu\text{m}$ ; flow rate: 0.3 mL/min; Phenomenex). Silica gel 60 (230–400 mesh; Merck, Darmstadt, Germany) was used for column chromatography. TLC was performed using pre-coated silica gel F254 and RP-C18 F254s plates (Merck), and spots were detected under UV light or by heating following spraying with anisaldehyde-sulfuric acid.

**4.2. Plant Material.** *P. eldarica* needles were collected in May and June 2018 from the Tabriz district of Iran, which was identified by one of the authors (H. Hamishehkar). A voucher specimen (no.4036) was deposited in the Herbarium of the Pharmacy Faculty, Tabriz University of Medical Sciences.

**4.3. Extraction and Isolation.** Finely ground *P. eldarica* needles were extracted in MeOH using a Soxhlet extractor for 6 h at 40 °C, and the extraction rate was 16%. The extracts were collected and filtered through Whatman filter paper no.1, and the filtrates were concentrated under vacuum at 35 °C using a rotary evaporator (Heidolph, Germany). The resulting crude MeOH extract (296.3 g) was suspended in distilled water (700 mL) and subjected to solvent partitioning with hexane, CH<sub>2</sub>Cl<sub>2</sub>, EtOAc, and *n*-BuOH (each 700 mL  $\times$  3), yielding its four corresponding solvent-partitioned fractions. Based on the LC–MS and TLC analyses of each fraction derived from solvent partitioning, we easily observed that the hexane-soluble fraction contains major non-polar compounds with characteristic colors indicating diterpenes following spraying with anisaldehyde-sulfuric acid via TLC analysis. The hexane-soluble fraction (19.9 g) was loaded onto a silica gel open column chromatography apparatus and fractionated using a gradient solvent system of hexane-EtOAc (30:1-1:1, *v/v*) to yield 13 subfractions (H1–H13). Subfraction H7 (260 mg) was further isolated by preparative HPLC (gradient solvent system from 80% MeOH/H<sub>2</sub>O to 100% MeOH) to yield five subfractions (H71–H75). Subfraction H72 (55 mg) was purified by semipreparative HPLC using an isocratic system of 77% MeOH/H<sub>2</sub>O, which further yielded four subfractions (H721–H724). Subfraction H721 (27.6 mg) was further purified by semipreparative HPLC with an isocratic system of 65% MeCN/H<sub>2</sub>O to yield compounds 3 (*t*<sub>R</sub> 19.5 min, 5.8 mg) and 1 (*t*<sub>R</sub> 21.0 min, 2.1 mg). Subfraction H73 (46 mg) was purified by semipreparative HPLC with an isocratic system of 87% MeOH/H<sub>2</sub>O to isolate compound 2 (*t*<sub>R</sub> 39.5 min, 1.0 mg).

**4.3.1. Eldaricoxide A (1).** Amorphous white powder; [ $\alpha$ ]<sub>D</sub><sup>25</sup>+8.9 (*c* 0.10, CHCl<sub>3</sub>); UV (MeOH)  $\lambda_{\text{max}}$  (log  $\epsilon$ ) 205 (0.88); CD (MeOH)  $\lambda_{\text{max}}$  ( $\Delta\epsilon$ ) 200 (−0.01), IR (KBr)  $\nu_{\text{max}}$ : 3065, 1638, 1283, 1115 cm<sup>−1</sup>; <sup>1</sup>H (850 MHz) and <sup>13</sup>C (212.5 MHz) NMR data, see Table 1; HR-ESIMS (positive-ion mode) *m/z* 331.2250 [*M* + Na]<sup>+</sup> (calcd for C<sub>19</sub>H<sub>32</sub>O<sub>3</sub>Na, 331.2249).

**4.4. ECD Calculation.** Initial conformational searches were performed in the MMFF94 force field using the MacroModel (version 2021-4, Schrödinger LLC) program with a mixed torsional/low-mode sampling method, in which a gas phase

with a 50 kJ/mol energy window and 10,000 maximum iterations was employed. The Polak–Ribiere conjugate gradient algorithm was established with 10,000 maximum iterations and a  $0.001 \text{ kJ} (\text{mol } \text{Å})^{-1}$  convergence threshold on the root-mean-square gradient to minimize conformers. The conformers proposed in this study (found within 5 kJ/mol in the MMFF force field) were selected for geometry optimization using TmoleX 4.3.2 with the density functional theory settings of B3-LYP/6-31+G (d,p).<sup>32</sup>

ECD calculations for the **1a** and **1b** conformers (six conformers each) were performed at an identical theoretical level and basis sets. The calculated ECD spectra were simulated by superimposing each transition, where  $\sigma$  is the bandwidth at height  $1/e$  and  $\Delta E_i$  and  $R_i$  are the excitation energy and rotatory strength for transition  $i$ , respectively.<sup>32</sup> In this study, the value of  $\sigma$  was 0.2 eV. The excitation energies and rotatory strengths of the ECD spectra were calculated based on the Boltzmann populations of the conformers, and ECD visualization was performed using SigmaPlot 14.0.

$$\Delta\epsilon(E) = \frac{1}{2.297 \times 10^{-39}} \frac{1}{\sqrt{2\pi\sigma}} \sum_A^i \Delta E_i R_i e^{[-(E-\Delta E_i)^2/(2\sigma)^2]}$$

**4.5. *H. pylori* Culture.** The clinical strain of *H. pylori* 51 (HPKTCC B0006) isolated from a Korean patient with a duodenal ulcer was provided by the *H. pylori* Korean Type Culture Collection, School of Medicine, Gyeongsang National University, Korea. The strain was cultured and maintained on Brucella agar (BD Co., Sparks, MD, USA) supplemented with 10% horse serum (Gibco, New York, USA). The culture conditions were 37 °C, 100% humidity, and 10% CO<sub>2</sub> for 2–3 days.

**4.6. Determination of Minimal Inhibitory Concentration (MIC) Values.** Minimal inhibitory concentrations (MICs) were determined using the broth dilution method as previously reported.<sup>33,34</sup> Twenty microliters of the bacterial colony suspension, equivalent to  $2-3 \times 10^8$  CFU/mL and 20  $\mu\text{L}$  of twofold diluted test samples and controls, respectively, was added to each well of a six-well plate containing Brucella broth medium supplemented with 10% horse serum. The final volume was made to 2 mL. After 24 h of incubation, the bacterial growth was evaluated by measuring the optical density at 600 nm using a spectrophotometer. The MIC<sub>50</sub> and MIC<sub>90</sub> values were defined as the lowest concentrations of samples at which bacterial growth was inhibited by 50 and 90%, respectively, and were computed using Microsoft Excel (Redmond, WA, USA). All values were obtained from two independent experiments.

## ■ ASSOCIATED CONTENT

### SI Supporting Information

The Supporting Information is available free of charge at <https://pubs.acs.org/doi/10.1021/acsomega.2c04147>.

HR-ESIMS and 1D and 2D NMR spectra of compound **1** (PDF)

## ■ AUTHOR INFORMATION

### Corresponding Authors

Jung Kyu Kim – School of Chemical Engineering, Sungkyunkwan University, Suwon 16419, Republic of Korea; [orcid.org/0000-0002-8218-0062](https://orcid.org/0000-0002-8218-0062); Phone: +82-31-290-7254; Email: [legkim@skku.edu](mailto:legkim@skku.edu)

Ki Hyun Kim – School of Pharmacy, Sungkyunkwan University, Suwon 16419, Republic of Korea; [orcid.org/0000-0002-5285-9138](https://orcid.org/0000-0002-5285-9138); Phone: +82-31-290-7700; Email: [khkim83@skku.edu](mailto:khkim83@skku.edu); Fax: +82-31-290-7730

### Authors

Se Yun Jeong – School of Pharmacy, Sungkyunkwan University, Suwon 16419, Republic of Korea

Myung Woo Na – School of Pharmacy, Sungkyunkwan University, Suwon 16419, Republic of Korea

Eon Chung Park – School of Pharmacy, Sungkyunkwan University, Suwon 16419, Republic of Korea

Jin-Chul Kim – KIST Gangneung Institute of Natural Products, Natural Product Informatics Research Center, Gangneung 25451, Republic of Korea

Dong-Min Kang – College of Pharmacy and Research Institute of Pharmaceutical Sciences, Gyeongsang National University, Jinju 52828, Republic of Korea

Hamed Hamishehkar – Drug Applied Research Center, Tabriz University of Medical Sciences, Tabriz 51656-65811, Iran

Mi-Jeong Ahn – College of Pharmacy and Research Institute of Pharmaceutical Sciences, Gyeongsang National University, Jinju 52828, Republic of Korea

Complete contact information is available at:

<https://pubs.acs.org/doi/10.1021/acsomega.2c04147>

### Author Contributions

#These authors contributed equally.

### Notes

The authors declare no competing financial interest.

## ■ ACKNOWLEDGMENTS

This work was supported by the National Research Foundation of Korea (NRF) grant funded by the Korean government (2019R1A5A2027340 and 2021R1A2C2007937) and the Korea Institute of Science and Technology intramural research grant (2E31881).

## ■ REFERENCES

- Michelozzi, M.; Tognetti, R.; Maggino, F.; Radicati, M. Seasonal variations in monoterpene profiles and ecophysiological traits in Mediterranean pine species of group "halepensis". *iForest* **2008**, *1*, 65–74.
- Alizadeh, M.; Safaie, N.; Shams-Bakhsh, M.; Mehrabadi, M. Neoscytalidium novaehollandiae causes dieback on *Pinus eldarica* and its potential for infection of urban forest trees. *Sci. Rep.* **2022**, *12*, 9337.
- Ghaffari, T.; Kafil, H. S.; Asnaashari, S.; Farajnia, S.; Delazar, A.; Baek, S. C.; Hamishehkar, H.; Kim, K. H. Chemical composition and antimicrobial activity of essential oils from the aerial parts of *Pinus eldarica* grown in Northwestern Iran. *Molecules* **2019**, *24*, 3203.
- Hames-Kocabas, E. E.; Yesil-Celiktas, O.; Isleten, M.; Vardar-Sukan, F. Antimicrobial activity of pine bark extract and assesment of potential application in cooked red meat. *Gida* **2008**, *33*, 123–127.
- Rohdewald, P. A review of the French maritime pine bark extract (Pycnogenol), a herbal medication with a diverse clinical pharmacology. *Int. J. Clin. Pharmacol. Ther.* **2002**, *40*, 158–168.
- Potta, S. P.; Doss, M. X.; Hescheler, J.; Sachinidis, A. Epigallocatechin-3-gallate (EGCG): A structural target for the development of potential therapeutic drugs against anti-proliferative diseases. *Drug Des. Rev.-Online* **2005**, *2*, 85–91.
- Li, K.; Li, Q.; Li, J.; Gao, D.; Zhang, T.; Han, Z.; Zheng, F. Effect of procyanidins from *Pinus koraiensis* bark on growth inhibition and

- expression of PCNA and TNF- $\alpha$  in mice with U14 cervical cancer. *Therapy* **2007**, *4*, 685–690.
- (8) Mamedov, N.; Craker, L. E. Medicinal plants used for the treatment of bronchial asthma in Russia and Central Asia. *J. Herbs, Spices Med. Plants* **2001**, *8*, 91–117.
- (9) Mamedov, N.; Gardner, Z.; Craker, L. E. Medicinal plants used in Russia and Central Asia for the treatment of selected skin conditions. *J. Herbs, Spices Med. Plants* **2005**, *11*, 191–222.
- (10) Iravani, S.; Zolfaghari, B. Phytochemical analysis of *Pinus eldarica* bark. *Res. Pharm. Sci.* **2014**, *9*, 243.
- (11) Hosseinzadeh, H.; Khooei, A. R.; Khashayarmanesh, Z.; Motamed-Shariaty, V. Antiuro lithiatic activity of *Pinus eldarica* medw: fruits aqueous extract in rats. *Urol. J.* **2010**, *7*, 232.
- (12) Huseini, H. F.; Anvari, M. S.; Rabbani, S.; Sharifi, F.; Arzaghi, S. M.; Fakhrzadeh, H. Anti-hyperlipidemic and anti-atherosclerotic effects of *Pinus eldarica* Medw. nut in hypercholesterolemic rabbits. *Daru, J. Pharm. Sci.* **2015**, *23*, 32.
- (13) Sadeghi, M.; Zolfaghari, B.; Jahanian-Najafabadi, A.; Abtahi, S. R. Anti-pseudomonas activity of essential oil, total extract, and proanthocyanidins of *Pinus eldarica* Medw. bark. *Res. Pharm. Sci.* **2016**, *11*, 58.
- (14) Sharifan, A.; Etebari, M.; Zolfaghari, B.; Aliomrani, M. Investigating the effects of bark extract and volatile oil of *Pinus eldarica* against cisplatin-induced genotoxicity on HUVECs cell line. *Toxicol. Res.* **2021**, *10*, 223–231.
- (15) Bolandghamat, S.; Moghimi, A.; Iranshahi, M. Effects of ethanolic extract of pine needles (*Pinus eldarica* Medw.) on reserpine-induced depression-like behavior in male Wistar rats. *Pharmacogn. Mag.* **2011**, *7*, 248.
- (16) Mansouri, S.; Hosseini, M.; Beheshti, F.; Sobhanifar, M. A.; Rakhshandeh, H.; Anaegoudari, A. Neuroprotective effects of *Pinus eldarica* in a mouse model of pentylentetrazole-induced seizures. *Avicenna J. Phytomed.* **2021**, *11*, 610.
- (17) Hajhashemi, V.; Zolfaghari, B.; Amin, P. Anti-nociceptive and anti-inflammatory effects of hydroalcoholic extract and essential oil of *Pinus eldarica* in animal models. *Avicenna J. Phytomed.* **2021**, *11*, 494.
- (18) Lee, S. R.; Kang, H.; Yoo, M. J.; Yu, J. S.; Lee, S.; Yi, S. A.; Kim, K. H. Anti-adipogenic pregnane steroid from a Hydractinia-associated fungus, *Cladosporium sphaerospermum* SW67. *Nat. Prod. Sci.* **2020**, *26*, 230–235.
- (19) Yu, J. S.; Park, M.; Pang, C.; Rashan, L.; Jung, W. H.; Kim, K. H. Antifungal phenols from *Woodfordia uniflora* collected in Oman. *J. Nat. Prod.* **2020**, *83*, 2261–2268.
- (20) Lee, S.; Ryoo, R.; Choi, J. H.; Kim, J. H.; Kim, S. H.; Kim, K. H. Trichothecene and tremulane sesquiterpenes from a hallucinogenic mushroom *Gymnopilus junonius* and their cytotoxicity. *Arch. Pharmacol. Res.* **2020**, *43*, 214–223.
- (21) Lim, S. H.; Yu, J. S.; Lee, H. S.; Choi, C. I.; Kim, K. H. Antidiabetic flavonoids from fruits of *Morus alba* promoting insulin-stimulated glucose uptake via Akt and AMP-activated protein kinase activation in 3T3-L1 adipocytes. *Pharmaceutics* **2021**, *13*, 526.
- (22) Lee, K. H.; Kim, J. K.; Yu, J. S.; Jeong, S. Y.; Choi, J. H.; Kim, J. C.; Ko, Y. J.; Kim, S. H.; Kim, K. H. Ginkwanghols A and B, osteogenic coumaric acid-aliphatic alcohol hybrids from the leaves of *Ginkgo biloba*. *Arch. Pharmacol. Res.* **2021**, *44*, 514–524.
- (23) Ha, J. W.; Kim, J.; Kim, H.; Jang, W.; Kim, K. H. Mushrooms: An important source of natural bioactive compounds. *Nat. Prod. Sci.* **2020**, *26*, 118–131.
- (24) Shaikh, R. U.; Dawane, A. A.; Pawar, R. P.; Gond, D. S.; Meshram, R. J.; Gacche, R. N. Inhibition of *Helicobacter pylori* and its associate urease by labdane diterpenoids isolated from *Andrographis paniculata*. *Phytother. Res.* **2016**, *30*, 412–417.
- (25) Edmond, M. P.; Mostafa, N. M.; El-Shazly, M.; Singab, A. N. B. Two clerodane diterpenes isolated from *Polyalthia longifolia* leaves: Comparative structural features, anti-histaminic and anti-*Helicobacter pylori* activities. *Nat. Prod. Res.* **2021**, *35*, 5282–5286.
- (26) Lee, C. K.; Fang, J. M.; Cheng, Y. S. Norditerpenes from *Juniperus chinensis* *Juniperus chinensis*. *Phytochemistry* **1995**, *39*, 391–394.
- (27) Ybarra, M. I.; Popich, S.; Borkosky, S. A.; Asakawa, Y.; Bardón, A. Manoyl Oxide Diterpenoids from *Grindelia scorzonifolia*. *J. Nat. Prod.* **2005**, *68*, 554–558.
- (28) Decorzant, R.; Vial, C.; Näf, F.; Whitesides, G. M. A short synthesis of ambrox from sclareol. *Tetrahedron* **1987**, *43*, 1871–1879.
- (29) Andersson, R.; Gref, R.; Lundgren, L. N. Manoyl oxide acid from resin of *Pinus sylvestris* needles. *Phytochemistry* **1990**, *29*, 1320–1322.
- (30) McGee, D. J.; George, A. E.; Trainor, E. A.; Horton, K. E.; Hildebrandt, E.; Testerman, T. L. Cholesterol enhances *Helicobacter pylori* resistance to antibiotics and LI-37. *Antimicrob. Agents Chemother.* **2011**, *55*, 2897–2904.
- (31) Chey, W. D.; Wong, B. C. American College of Gastroenterology Guideline on the Management of *Helicobacter pylori* Infection. *Am. J. Gastroenterol.* **2007**, *102*, 1808–1825.
- (32) Lee, S.; Kim, C. S.; Yu, J. S.; Kang, H.; Yoo, M. J.; Youn, U. J.; Ryoo, K. H.; Bae, H. Y.; Kim, K. H. Ergopyrone, a Styrylpyrone-Fused Steroid with a Hexacyclic 6/5/6/6/6/5 Skeleton from a Mushroom *Gymnopilus orientispectabilis*. *Org. Lett.* **2021**, *23*, 3315–3319.
- (33) Khalil, A. A. K.; Park, W. S.; Lee, J.; Kim, H. J.; Akter, K. M.; Goo, Y. M.; Bae, J. Y.; Chun, M. S.; Kim, J. H.; Ahn, M. J. A new anti-*Helicobacter pylori* juglone from *Reynoutria japonica*. *Arch. Pharmacol. Res.* **2019**, *42*, 505–511.
- (34) Amin, M.; Anwar, F.; Naz, F.; Mehmood, T.; Saari, N. Anti-*Helicobacter pylori* and urease inhibition activities of some traditional medicinal plants. *Molecules* **2013**, *18*, 2135–2149.